Eclética Química Journal

Original article

revista.iq.unesp.br

| Vol. 47 | n. 2 | 2022 |

Ni-Nb-Zr metastable phases formation, a thermodynamic and chemical approach

Leonardo Pratavieira Deo[1+]

1. Federal University of Lavras, Engineering Department, Lavras, Brazil.

+Corresponding author: Leonardo Pratavieira Deo, **Phone:** +55 (35) 3829-1860, **Email address:** leonardo.deo@ufla.br

ARTICLE INFO

Article history:
Received: October 22, 2021
Accepted: February 10, 2022
Published: April 01, 2022

Section Editor: Assis Vicente Benedetti

Keywords:
1. Ni-Nb-Zr alloy
2. no equilibrium phases
3. remnant stability

ABSTRACT: Gibbs' free energy of formation is considered a good guidance in order to describe or predict the phases formation within the standard state; however, many materials are produced out of their equilibrium conditions, and consequently, metastable phases are formed. There is no universal knowledge related to metastable phases formation; therefore, this paper presents considerations in order to elucidate some understanding about two metastable phases found in a rapid quenched alloy from Ni-Nb-Zr system during the solidification process. The analyzed alloy, namely $Ni_{61.6}Nb_{33.1}Zr_{5.3}$ (at.%) was previously synthesized and characterized in two previous works. The hypotheses presented here consider free energies of formation among phases which compete to nucleate, stability of crystalline phases at nanoscale and atomic pair preferences during the nucleation. The understanding related to metastable phases formation may produce and improve promising technological materials.

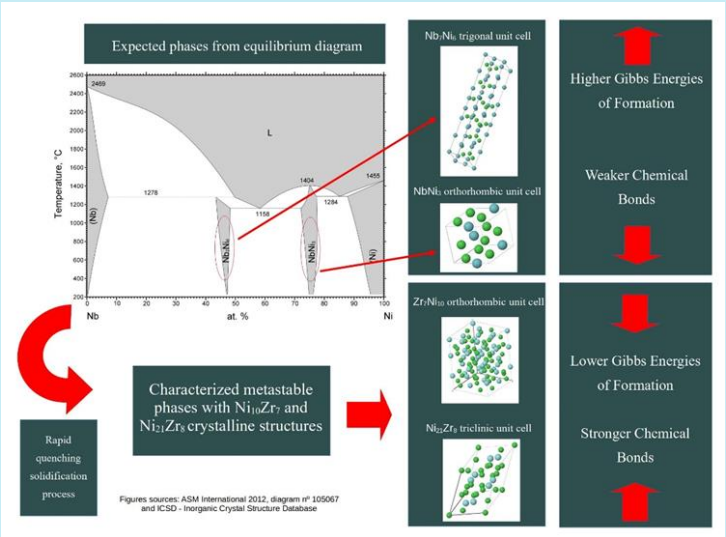

ISSN: 1678-4618
DOI: 10.26850/1678-4618eqj.v47.2.2022.p97-102

1. Introduction

Since the formulation of materials thermodynamics by Josiah Willard Gibbs in 1878 (Gibbs, 1878), one of the biggest paradigms in materials science and engineering has been the understanding about metastable materials and their phases (Sun *et al.*, 2016). According to Gibbs' theory, the constituent phases of materials have Gibbs free energy of formation (ΔfG°) values, which describes the quantity of energy necessary when a phase is formed from its constituent elements in their standard state. With changes in chemical composition, temperature and pressure, the ΔfG° of a phase varies and the most stable position is that one with the lowest value. The Gibbs free energy of formation also depends on other thermodynamics parameters, such as enthalpy and entropy of formation (Olivotos and Economou-Eliopoulos, 2016).

In contrast with stable phases, which are well described by Gibbs free energy of formation, in some especial manufacturing cases, metastable phases can be formed and they do not present the lowest free energy values. In other words, the metastable phases kinetically trap the stable phases with lower free energy values within the equilibrium state (Sun *et al.*, 2016). For numerous alloys, metastable phases can exhibit superior properties than their corresponding stable phases; examples can be found for metallic glasses, high entropy alloys and quenched steels (Hidalgo *et al.*, 2019; Kube and Schroers, 2020; Li *et al.*, 2016). Some mechanical properties of these alloys are their superior strength and hardness, excellent corrosion and wear resistance, as well as their general inability to undergo homogeneous plastic deformation (Trexler and Thadhani, 2010).

In this context, the present work presents a thermodynamics explanation about the crystallization of two metastable phases that developed in a rapid quenched alloy, namely $Ni_{61.6}Nb_{33.1}Zr_{5.3}$ (at.%), produced and characterized in previous works (Deo and Oliveira, 2014; 2017). According to the *liquidus* projection diagram of the Nb–Ni–Zr system calculated by Tokunaga *et al.* (2007), the expected equilibrium solidification crystalline phases for the analyzed alloy are the $NbNi_3$ and Nb_7Ni_6, both with some minor zirconium solubility; however, the previous characterization indicated a different crystallization behavior with non-equilibrium crystalline structures. The found structures were the same of the equilibrium $Ni_{10}Zr_7$ and $Ni_{21}Zr_8$ phases, in addition, with a large solubility of niobium in both structures, around 40 and 25 at.%, respectively (Deo and Oliveira, 2017).

In order to obtain some understanding about the non-equilibrium behavior of the analyzed alloy, some approach of the Gibbs energy of formation for each above-mentioned phase were calculated. The thermodynamic functions of formation expressed by Eqs. 1 and 2 for the Ni–Zr system were determined through reduction reactions examined with a Knudsen-cell mass spectrometer (Zaitsev *et al.*, 2002). Equations 3 and 4 were performed on the basis of the calculation of phase diagrams (CALPHAD) method for the Nb–Ni system (Tokunaga *et al.*, 2007). The Gibbs energy of formation of each phase per mole of formula unit are expressed by:

$$\Delta fG(Ni_{21}Zr_8) = -47028 + 5.99T, 1201 \leq T \leq 1438K \quad (1)$$

$$\Delta fG(Ni_{10}Zr_7) = -50075 + 5.16T, 1058 \leq T \leq 1339K \quad (2)$$

$$\Delta fG(NbNi_3) = -35300.6 + 4.83322T, 298 \leq T \leq 6000K \quad (3)$$

$$\Delta fG(Nb_6Ni_7) = -22770 + 0.305T, 298 \leq T \leq 6000K \quad (4)$$

Gibbs free energies of formation are relative values, not absolute, therefore this thermodynamic parameter allows to compare energies of different phases and only the individual values do not have physical significance. In addition, with the free energies of formation values, considerations were done about the stability of crystalline phases at nanoscale, as well as the atomic pair preferences during the nucleation. Therefore, the present paper presents some understanding about two metastable phases, which can be formed in the Ni–Nb–Zr system under a rapid solidification condition. The literature presents a lack of fundamental understanding related to metastable phases formation, even that metastable phases may yield promising new technological materials (Sun *et al.*, 2016).

2. Alloy confection and characterization and Gibbs energies of formation calculation

A rapid quenched wedge shape sample with maximum amorphous thickness of 3 mm was produced

Eclética Química Journal, vol. 47, n. 2, 2022, 97-102
ISSN: 1678-4618
DOI: 10.26850/1678-4618eqj.v47.2.2022.p97-102

by injection casting according to a procedure described in the previous work (Deo and Oliveira, 2014). The estimated cooling rate during the solidification process was around 250 K s^{-1}, therefore out of the equilibrium condition. In addition to the amorphous phase and metastable crystalline phases previously mentioned, the analyzed alloy shown the presence of unknown crystalline compounds not indexed by X-ray diffraction technique.

From transmission electron microscopy (TEM), the metastable phases present in the alloy microstructure were characterized by selected area electron diffraction (SAED), bright field (BF) images and energy dispersive X-ray (EDS) analysis. A transmission electron microscope with a tungsten source and an acceleration voltage of 120 kV coupled with an EDS detector was used to operate the TEM analysis. In addition, the X-ray diffraction (XRD) analysis was used as a complementary technique in order to confirm the phases previously identified by TEM. The diffraction analysis was carried out in a diffractometer with Cu Kα (1.5418 Å) radiation and the 2-theta varying from 20 to 70°.

In order to calculate the Gibbs energies of formation relative to each phase as presented by Eqs. 1–4, from another previous work (Deo and Oliveira, 2014), a differential scanning calorimetry (DSC) curve data was used to estimate the solidification temperature (1393 K) of the analyzed alloy. This DSC data is relative to an alloy chemical composition close to that analyzed in this paper. During the DSC experiment, the sample with weight around 40 mg was heated at a rate of 20 K min^{-1} from room temperature up to 1400 °C. DSC experiments are typically used to determine the characteristic temperatures of phase transformations, such as the solidification temperature. All detailed steps of sample characterization are described in previous works (Deo and Oliveira, 2014; 2017).

3. Thermodynamic hypothesis for metastable formation

The Gibbs energies of formation were calculated according to Eqs. 1–4 for the $Ni_{21}Zr_8$, $Ni_{10}Zr_7$, $NbNi_3$ and Nb_7Ni_6 phases, respectively, in the solidification temperature, 1393 K. Structural formulas, crystal systems and Gibbs energies values associated to each phase are shown in Tab. 1.

Table 1. Chemical, crystallographic and calculated thermodynamic parameters of phases.

Phase structural formula	Crystal system	Gibbs energy of formation calculated from solidification temperature (kJ mol^{-1})
$Ni_{21}Zr_8$ (Okamoto, 2007)	Triclinic (Joubert *et al.*, 1998)	–38.683
$Ni_{10}Zr_7$ (Okamoto, 2007)	Orthorhombic (Joubert *et al.*, 1997)	–42.887
$NbNi_3$ (Tokunaga *et al.*, 2007)	Orthorhombic (Fang *et al.*, 1992)	–28.567
Nb_7Ni_6 (Tokunaga *et al.*, 2007)	Trigonal (P. Nash and A. Nash, 1986)	–22.345

The Gibbs energy of formation values presented in Tab. 1 clearly show that $Ni_{21}Zr_8$ and $Ni_{10}Zr_7$ crystalline phases are thermodynamically preferred to be formed in the analyzed alloy when compared to $NbNi_3$ and Nb_7Ni_6 crystalline phases, once the first phases present lower values of Gibbs energy of formation. However, in contrast with this expectation, as reported by Matsumoto *et al.* (2005) in their calculated *liquidus* projection diagram of the Nb–Ni–Zr system, the $NbNi_3$ and Nb_7Ni_6 phases should be expected in the analyzed alloy, under equilibrium conditions during the solidification process.

The solidification always starts from a high-energy precursor, i.e., liquid phase, and there has not been a clear and detailed understanding of the effects causing the formation of the metastable structures from the viewpoint of thermodynamics, neither clear insight related to chemical and physical origins in order to lead to a tendency of metastable phases formation (C. Wang and Yang, 2005). Here, how surface energies and chemical composition may be related to the stabilization of metastable phases with $Ni_{21}Zr_8$ and $Ni_{10}Zr_7$ crystalline structures in the analyzed alloy is discussed.

First, the discussion is grouped around the influence of surface energies in order to form metastable phases. Before becoming a bulk crystalline material, all crystals first nucleate and grow in the nanoscale, where the contribution of surface energy is very significant. Small spherical crystalline particles with sizes larger or equal than 1/R (where R is the radius) can stabilize metastable crystalline polymorphic phases with low surface energies. Indeed, calorimetry experiments have demonstrated that metastable polymorphs can be stabilized at the nanoscale if they have lower surface energy than the stable phase (Navrotsky, 2004; 2011). These metastable phases can have the preferential nucleation instead of the equilibrium phases, once they

Eclética Química Journal, vol. 47, n. 2, 2022, 97-102
ISSN: 1678-4618
DOI: 10.26850/1678-4618eqj.v47.2.2022.p97-102

are thermodynamically stable at nanoscale because their lower surface energy can surpass the steady-state nucleation rate of the stable phase and consequently they have a lower nucleation barrier. This steady-state nucleation rate depends exponentially on this nucleation barrier, so minor differences in surface energy between polymorphs can correspond to orders of magnitude differences in nucleation rates, which can potentially result in bulk metastability (Sun *et al.*, 2015).

Thus, under the announced solidification experimental conditions in the analyzed alloy, the hypothesis is that, at nanoscale, the structures $Ni_{10}Zr_7$ and $Ni_{21}Zr_8$ from crystal systems orthorhombic and triclinic, respectively, must present lower nucleation barriers or surface energies than $NbNi_3$ and Nb_7Ni_6 structures from crystal systems orthorhombic and trigonal, respectively. In addition, with nucleation barrier concept, the stabilization of metastable phases also is intimately related to structure selection during nucleation (Sun *et al.*, 2015); however, the absolute values of these intermetallic compounds surface energies is not reported in literature yet. In a complementary way, the lower nucleation barrier concept associated to the metastable phases with structures $Ni_{10}Zr_7$ and $Ni_{21}Zr_8$ found in the analyzed alloy can be considered a remnant thermodynamic stability as evidenced by the Gibbs energy of formation values presented in Tab. 1.

The solidification always starts from the liquid, i.e., a supersaturated solution and metastable phases may nucleate with the lowest free energy at small sizes and low surface energies. After nucleation, the metastable nuclei may reduce their free energy by crystal growth, consuming the solute elements from liquid by atomic diffusion, in this case the niobium atoms, in order to form metastable solid solutions in $Ni_{10}Zr_7$ and $Ni_{21}Zr_8$ crystalline structures. As reported in a previous work (Deo and Oliveira, 2017), the niobium atomic radius is around 7% smaller than zirconium atomic radius, as well as, the mixing enthalpy for the Nb–Zr atomic pair has a positive value (4 kJ mol^{-1}). In this way, the Hume-Rothery rules provide some support for the solid solution formation. When the component atomic-size differences are less than 15%, in addition to positive or small negative values of enthalpy of mixing between elements, the formation of a substitutional solid solution is more feasible (Zhang *et al.*, 2008). This previous work also shows other experimental evidences about solid solution formations, such as EDS chemical compositions, peak shift in the XRD patterns and decrease in unit cell volumes and lattice parameters calculated from TEM data (Deo and Oliveira, 2017). Once the barrier to crystal growth is smaller than the barrier to nucleation of a new phase, the metastable phases may grow to a stabilized size. At this point, there is a thermodynamic driving force for a phase transformation from metastable to stable phases; however, the rapid quenching during the solidification process suppressed this transformation (Chen *et al.*, 2018). Thus, under thermodynamic equilibrium, it should be expected the formation of $NbNi_3$ and Nb_7Ni_6 crystalline phases with minor solid solubility of zirconium; however, due to the solidification condition, the metastable phases with $Ni_{10}Zr_7$ and $Ni_{21}Zr_8$ crystalline structures and large solubility of niobium were found.

4. Chemical hypothesis for metastable formation

Another complementary point of view about metastable phases formation is concerned to alloy chemical composition. The analyzed alloy has a higher amount of niobium than zirconium; however, the crystallized phases presented the crystalline structures like $Ni_{10}Zr_7$ and $Ni_{21}Zr_8$. This hypothesis about these unexpected crystalline structures is related to the larger negative value of mixing enthalpy between Ni-Zr and Ni-Nb atomic pairs than it is between Nb-Zr atomic pair. The mixing enthalpies for these atomic pairs are −49 (Ni–Zr),−30 (Ni–Nb) and 4 (Nb–Zr) kJ mol^{-1} (Yamaura *et al.*, 2005). When nucleation starts from the liquid, despite the large amount of niobium, the atomic pair Ni–Zr is preferred, conducting to $Ni_{10}Zr_7$ and $Ni_{21}Zr_8$ formation instead of $NbNi_3$ and Nb_7Ni_6.

According to J. Wang *et al.* (2021), the mixing enthalpy can be approximately the cohesive energy when the samples are exposed to an oscillation of external pressure during the solidification process. In addition, Sun *et al.* (2016) affirm that when the average cohesive energy for a given chemistry is stronger, greater is the possibility for crystalline metastability. In other words, when cohesive energy and consequently chemical bonds are stronger, it is possible to stabilize higher-energy atomic arrangements, allowing thermodynamically that metastable compounds resist the transformations to equilibrium states.

In addition, a liquid below solidus temperature is considered to be in a metastable/unstable equilibrium, and the strongest attractive interactions between specific atomic pairs are preferred in order to make up short-rang order domains (as quenched-in embryos) (Fan *et al.*, 2000). If nucleation is suppressed, the amorphous phase may be formed; however, if cooling

Eclética Química Journal, vol. 47, n. 2, 2022, 97-102
ISSN: 1678-4618
DOI: 10.26850/1678-4618eqj.v47.2.2022.p97-102

rate during the solidification process is not high enough to lead to the glassy phase, metastable crystalline phases with the strongest attractive interactions between specific atomic pairs can be nucleated and after growing up in the material, as evidenced in the analyzed alloy in a previous work (Deo and Oliveira, 2017).

4. Conclusions

The discussion above presents two complementary hypotheses in order to understand the reasons why two metastable phases were formed in an alloy from Ni–Nb–Zr system during a rapid quenching solidification process instead of the thermodynamic equilibrium phases. The first hypothesis is concerned about the stability of $Ni_{10}Zr_7$ and $Ni_{21}Zr_8$ crystalline phases at nanoscale, once they must present lower surface energies than other polymorphs, so these crystalline phases have a lower nucleation barrier. Metastable phases may present the nucleation rates with orders of magnitude higher then stable phases due their lower surface energies, conducting to bulk metastability, as observed in the analyzed alloy. In addition, the barrier to crystal growth is smaller than the barrier to nucleation, so the metastable solid solutions with large amount of niobium in $Ni_{10}Zr_7$ and $Ni_{21}Zr_8$ crystalline structures might grow to a stabilized size. The presence of these reported phases is in good agreement with Gibbs energy of formation values, once these phases presented lower values compared to that presented to the expected phases according to the *liquidus* projection diagram. The second hypothesis is related to stabilization of atomic arrangements due the highest bonding energy between their constituent elements, i.e., during crystalline phases nucleation, the atomic pair Ni–Zr was preferred, despite the large amount of niobium in the alloy composition, leading to $Ni_{10}Zr_7$ and $Ni_{21}Zr_8$ structures formation.

From the viewpoint of thermodynamics, there is no universal understanding why some metastable phases can be nucleated and grown; however, in this present analysis, the metastable nucleation happens under instantaneous local thermodynamic conditions (nuclei with low surface energies and low Gibbs energy of formation) and the growth happens through the reduction of free energy related to the phase transformation in the solidification process. Therefore, it is possible to suppose that metastability can be considered as a "kind of remnant stability", so if the remnant stability can be understood, the metastability also can be better understood as well. In addition, the metastable nucleation can also be associated with atomic chemical preferences in order to make preferential bonds in a system with several elements.

Authors' contribution

Conceptualization: Deo, L. P.
Data curation: Deo, L. P.
Formal Analysis: Deo, L. P.
Funding acquisition: Not applicable.
Investigation: Deo, L. P.
Methodology: Deo, L. P.
Project administration: Deo, L. P.
Resources: Deo, L. P.
Software: Not applicable.
Supervision: Deo, L. P.
Validation: Deo, L. P.
Visualization: Deo, L. P.
Writing – original draft: Deo, L. P.
Writing – review & editing: Deo, L. P.

Data availability statement

Data sharing is not applicable.

Funding

Not applicable.

Acknowledgments

Not applicable.

References

Chen, B.-R.; Sun, W.; Kitchaev, D. A.; Mangum, J. S.; Thampy, V.; Garten, L. M.; Ginley, D. S.; Gorman, B. P.; Stone, K. H.; Ceder, G.; Toney, M. F.; Schelhas, L. T. Understanding crystallization pathways leading to manganese oxide polymorph formation. *Nat. Commun.* **2018**, *9*, 2553. https://doi.org/10.1038/s41467-018-04917-y

Deo, L. P.; Oliveira, M. F. Accuracy of a selection criterion for glass forming ability in the Ni–Nb–Zr system. *J. Alloys. Compd.* **2014**, *615* (Suppl. 1), S23–S28. https://doi.org/10.1016/J.JALLCOM.2013.11.194

Deo, L. P.; Oliveira, M. F. Metastable Phases Found in the Ni-Nb-Zr System. *Mater. Charact.* **2017**, *127*, 60–63. https://doi.org/10.1016/j.matchar.2017.03.001

Fan, C.; Li, C.; Inoue, A. Nanocrystal composites in Zr–Nb–Cu–Al metallic glasses. *J. Non-Cryst. Solids.* **2000,** *270* (1–3), 28–33. https://doi.org/10.1016/S0022-3093(00)00078-8

Fang, T.; Kennedy, S. J.; Quan, L.; Hicks, T. J. The structure and paramagnetism of Ni_3Nb. *J. Phys. Condens. Matter.* **1992**, *4*, 2405. https://doi.org/10.1088/0953-8984/4/10/007

Gibbs, J. W. On the Equilibrium of Heterogeneous Substances. *Am. J. Sci.* **1878**, *96*, 3. https://doi.org/10.11588/heidok.00013220

Hidalgo, J.; Huizenga, R. M.; Findley, K. O.; Santofimia, M. J. Interplay between metastable phases controls strength and ductility in steels. *Mat Sci Eng A.* **2019**, *745*, 185–194. https://doi.org/10.1016/J.MSEA.2018.12.096

Joubert, J.-M.; Černý, R.; Yvon, K.; Latroche, M.; Percheron-Guégan, A. Zirconium-Nickel, Zr7Ni10: Space Group Revision for the Stoichiometric Phase. *Acta Crystallogr C.* **1997**, *C53*, 1536–1538. https://doi.org/10.1107/S0108270197007142

Joubert, J.-M.; R. Černý; Yvon, K.; Latroche, M.; Percheron-Guegan, A. Refinement of the Crystal Structure of Zirconium Nickel, Zr_8Ni_{21}. *Z. Krist-New Cryst. St.* **1998**, *213*, 227–228. https://doi.org/10.1524/NCRS.1998.213.14.227

Kube, S. A.; Schroers, J. Metastability in high entropy alloys. *Scr. Mater.* **2020**, *186*, 392–400. https://doi.org/10.1016/J.SCRIPTAMAT.2020.05.049

Li, Z., Pradeep, K. G.; Deng, Y.; Raabe, D.; Tasan, C. C. Metastable high-entropy dual-phase alloys overcome the strength–ductility trade-off. *Nature.* **2016**, *534*, 227–230. https://doi.org/10.1038/nature17981

Matsumoto, S.; Tokunaga, T.; Ohtani, H.; Hasebe, M. Thermodynamic Analysis of the Phase Equilibria of the Nb–Ni–Ti System. *Mater Trans.* **2005**, *46* (12), 2920–2930. https://doi.org/10.2320/MATERTRANS.46.2920

Nash, P.; Nash, A. The Nb−Ni (Niobium-Nickel) system. *Bull. Alloy. Phase Diagr.* **1986**, *7*, 124–130. https://doi.org/10.1007/BF02881547

Navrotsky, A. Energetic clues to pathways to biomineralization: Precursors, clusters, and nanoparticles. *Proc. Natl. Acad. Sci. U.S.A.* **2004**, *101* (33), 12096. https://doi.org/10.1073/PNAS.0404778101

Navrotsky, A. Nanoscale Effects on Thermodynamics and Phase Equilibria in Oxide Systems. *ChemPhysChem.* **2011**, *12* (12), 2207–2215. https://doi.org/10.1002/CPHC.201100129

Okamoto, H. Ni-Zr (Nickel-Zirconium). *J. Phase Equilib. Diffus.* **2007**, *28*, 409. https://doi.org/10.1007/S11669-007-9120-Z

Olivotos, S.; Economou-Eliopoulos M. Gibbs Free Energy of Formation for Selected Platinum Group Minerals (PGM). *Geosci.* **2016**, *6* (1), 2. https://doi.org/10.3390/GEOSCIENCES6010002

Sun, W.; Jayaraman, S.; Chen, W.; Persson, K. A.; Ceder, G. Nucleation of metastable aragonite $CaCO_3$ in seawater. *Proc. Natl. Acad. Sci. U.S.A.* **2015**, *112* (11), 3199–3204. https://doi.org/10.1073/PNAS.1423898112

Sun, W.; Dacek, S. T.; Ong, S. P.; Hautier, G.; Jain, A.; Richards W. D.; Gamst A. C.; Persson K. A.; Ceder, G. The thermodynamic scale of inorganiccrystalline metastability. *Sci. Adv.* **2016**, *2* (11), e1600225. https://doi.org/10.1126/SCIADV.1600225

Tokunaga, T.; Matsumoto, S.; Ohtani, H.; Hasebe, M. Thermodynamic Analysis of the Phase Equilibria in the Nb-Ni-Zr System. *Mater. Trans.* **2007**, *48* (9), 2263–2271. https://doi.org/10.2320/matertrans.MB200713

Trexler, M. M.; Thadhani N. N. Mechanical properties of bulk metallic glasses. *Prog. Mater. Sci.* **2010**, *55* (8), 759–839. https://doi.org/10.1016/J.PMATSCI.2010.04.002

Wang, C. X.; Yang, G. W. Thermodynamics of metastable phase nucleation at the nanoscale. *Mater. Sci. Eng. R Rep.* **2005**, *49* (6), 157–202. https://doi.org/10.1016/J.MSER.2005.06.002

Wang, J.; Qin, J.; Zhou, J.; Cheng, K., Zhan, C.; Zhang, S.; Zhao, G.; Li, X.; Shen, K; Zhou, Y. Correlation between mixing enthalpy and structural order in liquid Mg−Si system. *T. Nonferr. Metal. Soc.* **2021**, *31* (3), 853–864. https://doi.org/10.1016/S1003-6326(21)65544-9

Yamaura, S.; Sakurai, M.; Hasegawa, M.; Wakoh, K.; Shimpo, Y.; Nishida, M.; Kimura, H.; Matsubara, E.; Inoue, A. Hydrogen permeation and structural features of melt-spun Ni–Nb–Zr amorphous alloys. *Acta Mater.* **2005**, *53* (13), 3703–3711. https://doi.org/10.1016/j.actamat.2005.04.023

Zaitsev, A. I.; Zaitseva, N. E.; Shakhpazov E. K.; Kodentsov, A. A. Thermodynamic Properties and Phase Equilibria in the Nickel–Zirconium System. The Liquid to Amorphous State Transition. *Phys. Chem. Chem. Phys.* **2002**, *4* (24), 6047–6058. https://doi.org/10.1039/B201036B

Zhang, Y.; Zhou,Y. J.; Lin, J. P.; Chen, G. L.; Liaw, P. K. Solid-Solution Phase Formation Rules for Multi-Component Alloys. *Adv. Eng. Mater.* **2008**, *10* (6), 534–538. https://doi.org/10.1002/adem.200700240

Eclética Química Journal, vol. 47, n. 2, 2022, 97-102
ISSN: 1678-4618
DOI: 10.26850/1678-4618eqj.v47.2.2022.p97-102